# Analysis of Coplanar Intermediate Coil Structures in Inductive Power Transfer Systems

Abhilash Kamineni, *Student Member, IEEE*, Grant A. Covic, *Senior Member, IEEE*, and John T. Boys

***Abstract*—Intermediate couplers have been shown to increase the coupling from primary to secondary pads in inductive power transfer (IPT) systems. This paper investigates embedding a coplanar intermediate coupler coil with the primary coil inside the primary pad to boost the coupling to the secondary pad and improve the efficiency of the system. Several coil designs are simulated and a mathematical model is developed to evaluate the efficiency of parallel–parallel and series–series tuned systems. As shown a coplanar, independently tuned intermediate coupler coil improves the efficiency of a series–series-tuned system since it reduces source losses. However, there appears to be no benefit to having an intermediate coupler with a parallel–parallel-tuned system. Furthermore, boosts in coupling are a result of adding extra current carrying windings to the primary pad and simulations show that operating the system as a traditional two coil IPT system may be simpler and more effective based on tuning topology. An experimental system was constructed to validate the simulations.**

***Index Terms*—Efficiency optimization, inductive power transfer, three coil resonator.**

## I. Introduction

INDUCTIVE power transfer (IPT) has allowed transfer of power wirelessly over a large air gap and is being proposed as a way of allowing electric vehicles (EVs) to charge without having to plug them into an outlet [1]–[6]. The efficiency of this system is largely dependent on the coupling between the primary and secondary pads. In EV charging applications the primary pad in the ground and the secondary pad under a car are separated by a varying air gap resulting in typical couplings ranging from 0.1–0.3.

Introducing a tuned intermediate coupler coil between the primary and secondary coils has been shown to boost the coupling and increase the transfer range [7]–[20]. However, having an intermediate coupler floating in midair is impractical for EV charging. Recent studies have investigated moving the intermediate coupler closer to the primary pad as well as finding the optimal frequency to tune the intermediate coupler [7]–[9]. The two coils can even rest inside each other in a coplanar arrangement [8], [13], [17], [18] or have a single turn primary winding that couples to an independently tuned winding with several turns [21]. These intermediate coupler structures have been reported as resulting in higher system efficiencies due to a boost in coupling factor of the secondary pad [8]–[12] but have not taken into account the benefits of adding extra copper to the system which boosts magnetic flux generation in the air gap.

An intermediate coupler coil can be embedded into the primary pad by winding the primary coil and this intermediate coupler coil in a coplanar fashion [8]. However since the intermediate coupler coil is in close proximity to the power supply, it can either be tuned independently and allowed to resonate on its own, or it can be connected in series with the primary coil and driven directly from the power supply. By doing this the total volume of copper in the primary pad is kept the same and a similar NI used, allowing the benefits of having an independently tuned intermediate coupler to be compared with a standard two coil IPT system. During the course of this study the benefits of such an intermediate coupler with a series–series-tuned system was published in [13], showing that this approach helped limit the impact of the source resistance. However, the mathematical model presented in [13] assumes ideal tuning such that all the coil reactances effectively cancel enabling simplified equations that can be compared easily between two coil and three coil equivalent structures to be obtained. Previous models for these systems presented in the literature have also made assumptions due to the complexity of equations taking into account several inductances and coupling factors. Some models ignore the coupling from primary to secondary coils [13], [20], [21] while other models assume that the coupling factor from primary and intermediate coupler coils to the secondary coil is equal [7] or combine several coupling factors into one fixed value [8]. However, these assumptions are not valid for all the intermediate coil structures that will be simulated in this study requiring a full model which takes into account all inductances and coupling factors. Consequently, the study presented in this paper takes a more general approach and investigates both parallel–parallel and series–series tuned systems along with the effects of mistuning, all of which requires a new mathematical model to be developed. Complete equations are developed to convert the system parameters of the three coil system including the independently tuned intermediate coupler into an equivalent set of system parameters for an equivalent two coil IPT system. This then allows the benefits of the three coil IPT system to be compared to a two coil IPT system by comparing the magnetic efficiency of the pads under both parallel–parallel and series–series tuning. The equivalency between certain parallel–parallel-tuned systems is also demonstrated.

The presented models are then validated with simulation and measurement. Here, 420-mm diameter circular pads, as described in [22], are used for both the primary and secondary. The

Manuscript received August 21, 2014; revised October 20, 2014; accepted November 22, 2014. Date of publication December 4, 2014; date of current version July 10, 2015. Recommended for publication by Associate Editor C. K. Lee.

The authors are with the Power Electronics Research Group, University of Auckland, Auckland 1142, New Zealand (e-mail: akam024@aucklanduni.ac.nz; ga.covic@auckland.ac.nz; j.boys@auckland.ac.nz).

Color versions of one or more of the figures in this paper are available online at http://ieeexplore.ieee.org.

Digital Object Identifier 10.1109/TPEL.2014.2378733

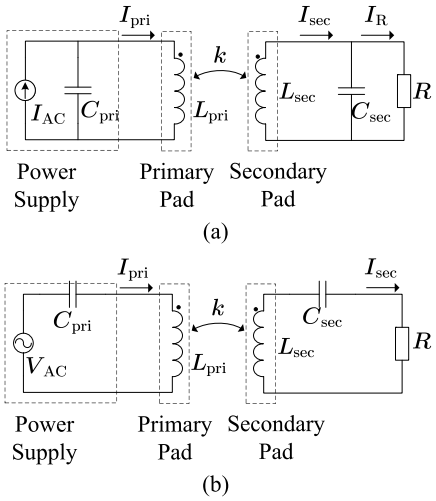


Fig. 1. Basic two coil IPT system with (a) parallel–parallel tuning and (b) series–series tuning.

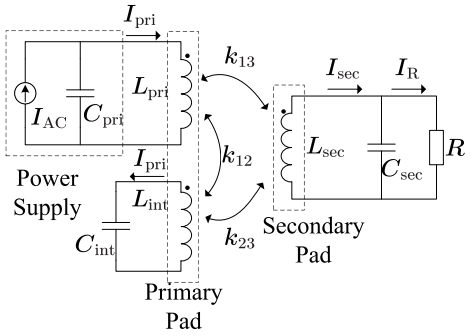


Fig. 2. Three coil, parallel–parallel IPT system with coplanar intermediate coupler in the primary pad.

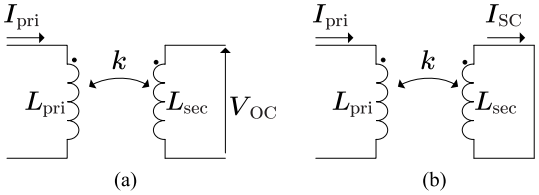


Fig. 3. Measuring the (a) open-circuit voltage ($V_{\rm OC}$) and (b) the short-circuit current ($I_{\rm SC}$).

original primary coil is replaced by 62 different coplanar primary and intermediate coupler coil structures with each design evaluated using JMAG—a 3-D FEM magnetic simulation software. JMAG has been shown to give reliable simulation results in past studies [22]. The best structure was then selected and built for comparison.

The structure of this paper is as follows. First, the fundamental equations of IPT systems will be derived in Section II. Then, a mathematical and magnetic simulation will be developed in Section III followed by an analysis of the optimal tuning in Section IV. In Section V, the efficiency of a parallel–parallel-tuned intermediate coupler system will be considered followed by the same analysis for a series–series-tuned system in Section VI. Section VII will discuss some practical considerations and Section VIII will show experimental results followed by some conclusions in Section IX.

## II. IPT Fundamentals

### A. Derivation of Fundamental Equations

The basic structure of an ideal parallel–parallel and series–series tuned two coil IPT system is shown in Fig. 1(a) and (b), respectively. The primary coil $L_{\rm pri}$ and secondary coil $L_{\rm sec}$ are tuned using capacitors $C_{\rm pri}$ and $C_{\rm sec}$ in both systems. The two coils are magnetically linked by coupling factor $k$ and are typically tuned to $\omega$—the driving frequency of the AC source $V_{\rm AC}$. If it is assumed that the reflected impedance of the secondary coil is low since $k$ is small, $V_{\rm AC}$ will see a resistive load at its terminals equivalent to the load R. Parallel-tuned primaries are often shown to be driven by a current source such as in Fig. 1(a). This is to ensure the voltage across $C_{\rm pri}$ does not change suddenly during switching in practical circuits.

An ideal three coil system which includes the intermediate coupler coil ($L_{\rm int}$) within the confines of the primary pad is shown in Fig. 2 where $L_{\rm int}$ is tuned by $C_{\rm int}$. Previous studies have suggested that the three coils would be tuned to frequencies different to the driving frequency [7], [8]. In this study, it is assumed that only $L_{\rm sec}$ is tuned to the driving frequency as discussed in Section IV. Since $L_{\rm pri}$, $L_{\rm int}$ and $L_{\rm sec}$ are all magnetically linked, two extra coupling factors $k_{12}$ and $k_{23}$ are introduced to the system. To accommodate these changes, the coupling factor $k$ from Fig. 1 has also been renamed $k_{13}$ in Fig. 2. An intermediate coupler can be added to a series–series system in a similar fashion shown in Fig. 2.

The open-circuit voltage ($V_{\rm OC}$) and short-circuit current ($I_{\rm SC}$) shown in Fig. 3(a) and (b), respectively, can be described as follows:

$$V_{\rm oc} = -j\omega k I_{\rm pri}\sqrt{L_{\rm pri}L_{\rm sec}} \tag{1}$$

$$I_{\rm sc} = \frac{V_{\rm OC}}{j\omega L_{\rm sec}} = \omega k I_{\rm pri}\sqrt{\frac{L_{\rm pri}}{L_{\rm sec}}}. \tag{2}$$

By using (1) and (2) and applying Norton's theorem to the parallel-tuned secondary, the output power is given by

$$P_{\rm out} = V_{\rm OC} I_{\rm SC} Q = \omega L_{\rm pri} I_{\rm pri}^2 k^2 Q \tag{3}$$

where $Q$ is the loaded quality factor of the tuned circuit (not to be confused with the quality factor of a coil) and is given by $Q = \frac{R}{\omega L_{\rm sec}}$.

Similarly, an expression for the output power of a three coil system is given by

$$P_{\rm out} = \omega\big(k_{13}^2 I_{\rm pri}^2 L_{\rm pri} + k_{23}^2 I_{\rm int}^2 L_{\rm int} + 2k_{13}k_{23}\sqrt{L_{\rm pri}L_{\rm int}} I_{\rm pri} I_{\rm int}\big)Q. \tag{4}$$

The same equations as (3) and (4) can be derived for a series–series system however the loaded circuit $Q$ is now defined as $Q = \frac{\omega L_{\rm sec}}{R}$.

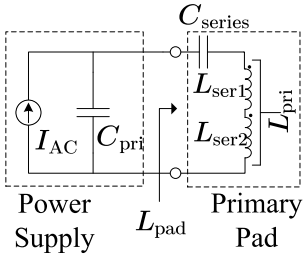


Fig. 4. Partial series compensation of $L_{\text{pri}}$ for parallel-tuned primaries.

Using (3) two coil systems can be compared by keeping $Q$ fixed and driving both primary pads with the same amount of input vars, assuming that reflected impedances are low. The system with the highest output power has the highest coupling and therefore the highest efficiency. However, in a three coil system, the output power is not just a function of the input vars, due to the extra term $2k_{13}k_{23}\sqrt{L_{\text{pri}}L_{\text{int}}}I_{\text{pri}}I_{\text{int}}$ in (4). This means that a three coil system cannot be compared to a two coil system by keeping the input vars constant. The simplest way to compare two coil and three coil systems is to look at the total efficiency of both systems while delivering the same output power.

### B. Series Compensation of Primary Coils

In the literature, it has been shown that the apparent coupling to a secondary pad increases when a coplanar intermediate is used [7], [8]. In fact, an equivalent of a coplanar primary pad structure is found in partially series-compensated parallel–parallel-tuned two coil systems where the apparent coupling also appears to increase. Here, it is often necessary to constrain the inductance of the primary coil by adding a series compensation capacitor $C_{\text{series}}$ without modifying the magnetic structure of the pad as shown in Fig. 4. This may be because the tuning capacitor $C_{\text{pri}}$ inside the power supply is fixed so the power supply is only able to drive a particular inductance. However, the most common reason is to manage the AC voltages across the windings since driving a large inductance with a large, high frequency AC current causes large voltages to build up in between windings causing arcing between neighboring windings.

In Fig. 4, part of the primary pad inductance $L_{\text{ser1}}$ is tuned out by $C_{\text{series}}$ so the effective inductance of the pad ($L_{\text{pad}}$) has decreased from $L_{\text{pri}}$ to $L_{\text{ser2}}$. Looking into the terminals of the pad ($L_{\text{pad}}$), it now requires lower input vars to achieve the same output power since $L_{\text{pad}}$ is lower than $L_{\text{pri}}$. If there was no knowledge about the addition of $C_{\text{series}}$ it would appear that the coupling factor has increased using (3). However, this is incorrect because the magnetic structure of the system has remained unchanged so the real coupling factor is the same.

## III. Development of Model

In this section, a mathematical model is developed for a parallel–parallel-tuned system. This model is then modified in Section VI to represent a series–series system.

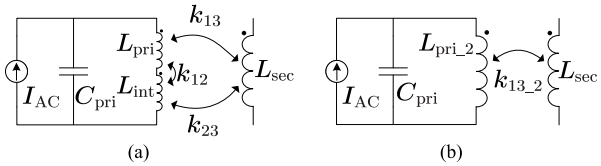


Fig. 5. (a) Driving the primary pad as a two coil system and (b) two coil equivalent circuit.

### A. Two Coil Equivalent System Model

To have a fair comparison between two coil and three coil systems, both structures must have the same volume of copper in the primary and secondary side. This separates the benefits of adding extra copper to the primary pad from the benefits of having an independently tuned intermediate coupler. This is done by driving $L_{\text{pri}}$ and $L_{\text{int}}$ in series as shown in Fig. 5(a) when simulating a two coil system, resulting in the primary pad having one coil ($L_{\text{pri\_2}}$) and the secondary pad having one coil ($L_{\text{sec}}$) as shown in Fig. 5(b).

Since $L_{\text{pri}}$ and $L_{\text{int}}$ are simply two mutually coupled inductors in series, $L_{\text{pri\_2}}$ is simply defined as

$$L_{\text{pri\_2}} = L_1 + L_2 + 2k_{12}\sqrt{L_1 L_2}. \tag{5}$$

The equivalent two coil system coupling factor can be found by equating the open-circuit voltage of the three coil system with the open-circuit voltage of the two coil equivalent system as shown

$$\begin{aligned} j\omega I_{\text{pri}}k_{13}\sqrt{L_{\text{pri}}L_{\text{sec}}} + j\omega I_{\text{pri}}k_{23}\sqrt{L_{\text{int}}L_{\text{sec}}} \\ = j\omega I_{\text{pri}}k_{13\_2}\sqrt{L_{\text{pri\_2}}L_{\text{sec}}}. \end{aligned} \tag{6}$$

This equation can be simplified to give

$$k_{13\_2} = \frac{k_{13}\sqrt{L_1} + k_{23}\sqrt{L_2}}{\sqrt{L_{\text{pri\_2}}}}. \tag{7}$$

### B. Steady-State Model for Parallel–Parallel Systems

The three coil system can be compared with its two coil equivalent system by comparing the efficiencies of the two systems. Here, the pad and source losses must both be considered because the pad losses tend to be the highest in an IPT system whereas the source losses become significant only when considering series–series systems as indicated in [7]. Capacitor losses on the other hand are significantly lower due to the high quality polypropylene tuning capacitors and as such these have been neglected for simplicity. This section will show the development of a mathematical model which considers pad losses for a parallel–parallel system. Section III-C will add the source to the system and Section VI will modify the model for series–series-tuned systems.

The three coil system and its two coil equivalent which will be modeled are shown in Fig. 6(a) and (b). Here, $r_{1\_2}$ in the two coil model is the sum of $r_1$ and $r_2$. $L_{1\_2}$ and $k_{13\_2}$ are the equivalent two coil system parameters derived using (5) and (7).

For this evaluation, the primary tuning capacitance ($C_1$) in both systems is assumed to automatically adjust itself so that the

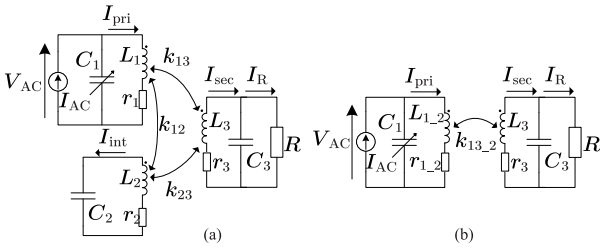


Fig. 6. (a) Three coil system with magnetic losses and (b) its two coil equivalent system.

impedance seen by the supply $V_{\rm AC}$ is always purely resistive. In practice, this can be achieved by using a "self-tuning" converter (a description of which will be developed in a following paper). $L_2$ and $C_2$ are tuned to frequency $f_2$ (angular frequency $\omega_2$) while $L_3$ and $C_3$ are tuned to frequency $f_3$ (angular frequency $\omega_3$). The power supply is assumed to operate at a constant driving frequency $f$ (angular frequency $\omega$) and the effects of bifurcation are ignored due to operation at low secondary $Q$ factors. All the results presented in this paper have $f$ fixed at 85 kHz.

By applying Kirchoff's voltage law to each tuned coil in Fig. 6(a), the following equations can be derived:

$$\begin{aligned} V_{\rm AC} = {} & (j\omega L_1 + r_1)\, I_{\rm pri} - j\omega k_{12}\sqrt{L_1 L_2} I_{\rm int} \\ & - j\omega k_{13}\sqrt{L_1 L_3} I_{\rm sec} \qquad (8) \\ 0 = {} & j\omega k_{12}\sqrt{L_1 L_2} I_{\rm pri} + \left(j\omega L_2 + \frac{1}{j\omega C_2} + r_2\right) I_{\rm int} \\ & - j\omega k_{23}\sqrt{L_2 L_3} I_{\rm sec} \qquad (9) \\ 0 = {} & j\omega k_{13}\sqrt{L_1 L_3} I_{\rm pri} - j\omega k_{23}\sqrt{L_2 L_3} I_{\rm int} \\ & + \left(j\omega L_3 + \frac{1}{j\omega C_3 + \frac{1}{R}} + r_3\right) I_{\rm sec} \qquad (10) \end{aligned}$$

where $C_2 = \frac{1}{\omega_2^2 L_2}$, $C_3 = \frac{1}{\omega_3^2 L_3}$ and $R = \omega L_3 Q$.

These equations can be rewritten in matrix form

$$\begin{bmatrix} \frac{V_{AC}}{j\omega L_1} \\ 0 \\ 0 \end{bmatrix} = \begin{bmatrix} a_1 & -k_{12}\sqrt{\frac{L_2}{L_1}} & -k_{13}\sqrt{\frac{L_3}{L_1}} \\ k_{12}\sqrt{\frac{L_1}{L_2}} & a_2 & -k_{23}\sqrt{\frac{L_3}{L_2}} \\ k_{13}\sqrt{\frac{L_1}{L_3}} & -k_{23}\sqrt{\frac{L_2}{L_3}} & a_3 \end{bmatrix} \begin{bmatrix} I_{\rm pri} \\ I_{\rm int} \\ I_{\rm sec} \end{bmatrix} \qquad (11)$$

where $a_1 = 1 + \frac{r_1}{j\omega L_1}$, $a_2 = -\left(1 - \frac{\omega_2^2}{\omega^2}\right) - \frac{r_2}{j\omega L_2}$ and $a_3 = -\left(1 + \frac{1}{-\frac{\omega^2}{\omega_3^2} + \frac{j}{Q}}\right) - \frac{r_3}{j\omega L_3}$.

Similarly, we can show that a two coil equivalent system in Fig. 6(b) can be represented in matrix form

$$\begin{bmatrix} \frac{V_{\rm AC}}{j\omega L_{1\_2}} \\ 0 \end{bmatrix} = \begin{bmatrix} a_{1\_2} & -k_{13\_2}\sqrt{\frac{L_3}{L_{1\_2}}} \\ k_{13\_2}\sqrt{\frac{L_{1\_2}}{L_3}} & a_3 \end{bmatrix} \begin{bmatrix} I_{\rm pri\_2} \\ I_{\rm sec} \end{bmatrix} \qquad (12)$$

where $a_{1\_2} = 1 + \frac{r_{1\_2}}{j\omega L_{1\_2}}$.

The variables $a_1$, $a_2$ and $a_3$ represent the effects of tuning to different frequencies as well as the effects of system losses and output loading. The assumption that $V_{\rm AC}$ always drives a purely resistive load can be seen by the fact that $a_1$ is independent of any tuning frequency terms. Solving (11) gives the following set of useful equations to describe a parallel–parallel-tuned three coil system:

$$\left.\begin{aligned} V_{\rm AC} &= j\omega L_1 I_{\rm pri}\,(a_1 + k_{V\,\rm AC}) \\ I_{\rm sec} &= -\frac{k_{12}k_{23} + a_2 k_{13}}{a_2 a_3 - k_{23}^2}\sqrt{\frac{L_1}{L_3}} I_{\rm pri} \\ I_{\rm int} &= -\frac{k_{13}k_{23} + a_3 k_{12}}{a_2 a_3 - k_{23}^2}\sqrt{\frac{L_1}{L_2}} I_{\rm pri} \\ VA_{\rm pri} &= j\omega L_1 \left|I_{\rm pri}\right|^2 (a_1 + k_{V\,\rm AC}) \\ VA_{\rm int} &= j\omega L_2\,(1 + a_2)\left|I_{\rm int}\right|^2 \\ VA_{\rm sec} &= j\omega L_3\,(1 + a_3)\left|I_{\rm sec}\right|^2 \end{aligned}\right\} \qquad (13)$$

where $k_{V\,\rm AC} = \dfrac{a_2 k_{13}^2 + a_3 k_{12}^2 + 2k_{12}k_{23}k_{23}}{a_2 a_3 - k_{23}^2}$.

Similarly, (12) can be solved to give the following set of useful equations to describe a parallel–parallel-tuned two coil equivalent system:

$$\left.\begin{aligned} V_{\rm AC} &= j\omega L_{1\_2} I_{\rm pri\_2}\left(a_{1\_2} + \tfrac{k_{13\_2}^2}{a_3}\right) \\ I_{\rm sec\_2} &= -\tfrac{k_{13\_2}}{a_3}\sqrt{\tfrac{L_1}{L_3}} I_{\rm pri\_2} \\ VA_{\rm pri\_2} &= j\omega L_1 \left|I_{\rm pri\_2}\right|^2 \left(a_{1\_2} + \tfrac{k_{13\_2}^2}{a_3}\right) \\ VA_{\rm sec\_2} &= j\omega L_3\,(1 + a_3)\left|I_{\rm sec\_2}\right|^2. \end{aligned}\right\} \qquad (14)$$

The currents are expressed in terms of $I_{\rm pri}$ and $I_{\rm pri\_2}$ instead of in terms of $V_{\rm AC}$ for convenience. The equations for $VA_{\rm int}$, $VA_{\rm sec}$ and $VA_{\rm sec\_2}$ are not used in this paper but are included for completeness. (11)–(14) are applicable to any three coil IPT system, regardless of the location of the intermediate coil, and not just the coplanar intermediate coil structures studied in this paper.

The equations for *VA* in (13) and (14) show the *VA* of the coil (including the effects of any reflected impedances and the losses) measured across the terminals of that coil. The output power of each system can be calculated by using

$$P_{\rm out} = \left|\frac{I_{\rm sec}}{1 + j\omega^2/\omega_3^2}\right|^2 R = I_R^2 R \qquad (15)$$

and the efficiency of either system can be given by

$$\eta = \frac{P_{\rm out}}{\Re\left(VA_{\rm pri}\right)}. \qquad (16)$$

### C. Source Resistance Modeling

Source resistance is used to model the losses in the components that generate the AC current in the power supply. In a real system it would model the losses in the H-bridge converter and gate driving circuitry. The source loss is important to consider for series-tuned power supplies since the H-bridge has to provide the vars to drive the track. This can be seen in Fig. 7(a) where the primary coil current $I_{\rm pri}$ flows through the source $V_{\rm AC}$

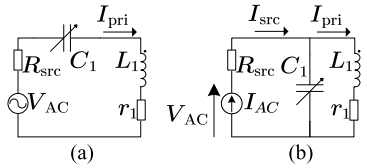


Fig. 7. Source resistance for (a) series-tuned primary systems and (b) parallel-tuned primary systems.

resulting in large source losses. However, with a parallel-tuned primary system, the large track current is created by a resonant LC tank as shown in Fig. 7(b) and therefore the source loss has much less impact given the power supply only provides the real power necessary to drive the load and overcome other losses, resulting in a lower source current $I_{\rm src}$ and therefore lower source losses compared to a series-tuned power supply.

For this study, it is assumed that an H-bridge is driven by an ideal dc source with ideal gate driving circuitry. The main losses in an H-bridge are the conduction losses and switching losses. The conduction losses in an H-bridge are given by

$$P_C = 2R_{\rm on}I_{\rm src}^2 \tag{17}$$

where $R_{\rm on}$ is the on state resistance of one switch.

In this analysis switching losses can be assumed to be negligible compared to the conduction losses. This is because the circuit is effectively zero current switched since the inductor and its reflected impedances are perfectly tuned out by $C_{\rm pri}$. In practice, this is verified by a previous study which used a similar converter and found that the switching losses were only 20% of the total H-bridge losses [23]. Even if the primary coil was slightly mistuned, as is normally done to avoid the effects of bifurcation in series-tuned primary coils, the maximum switching loss of a power MOSFET can be approximated to within 30% [24] by

$$P_{\rm SW} = \frac{1}{2}I_D V_D (t_{\rm OFF} + t_{\rm ON}) f \tag{18}$$

where $I_D$ and $V_D$ are the drain current and drain voltage of the switch at the moment of switching, $t_{\rm on}$ and $t_{\rm off}$ are the turn-on and turn-off times of the MOSFET and $f$ is the switching frequency. This suggests that the switching loss is proportional to the power being delivered by the H-bridge. In this study, the output power is always held constant at 1 kW in all the situations explored so any switching losses will be approximately constant and hence can be ignored in the comparisons.

The source resistance can therefore be approximated as

$$r_{\rm src} = 2R_{\rm on}. \tag{19}$$

Since $R_{\rm on}$ is dependent on the quality of the MOSFETs used, simulations will be run at $r_{\rm src} = 0$, 0.08 and 0.2 Ω. This allows the system to be evaluated with no source resistance, as well as allowing the trend of varying source losses to be observed.

The efficiency of the system, including the source losses, can then be calculated as

$$\eta = \frac{P_{\rm out}}{r_{\rm src}I_{\rm src}^2 + \Re\left(VA_{\rm pri}\right)}. \tag{20}$$

TABLE I
PARAMETERS USED TO VALIDATE MATHEMATICAL MODEL

| | | | |
|---|---|---|---|
| $L_1$ | 10.45 $\mu$H | $r_1$ | 0.0495 mΩ |
| $L_2$ | 32.31 $\mu$H | $r_2$ | 0.0815 mΩ |
| $L_3$ | 66.51 $\mu$H | $r_3$ | 0.1310 mΩ |
| $C_1$ | 151.4 nF | $k_{12}$ | 0.6165 |
| $C_2$ | 83.18 nF | $k_{13}$ | 0.1145 |
| $C_3$ | 51.55 nF | $k_{23}$ | 0.1292 |
| $V_{\rm AC}$ amplitude | 289.7 V | $R_{\rm src}$ | 0.08 Ω |
| $R$ | 177.6 Ω | $f$ | 85000 |

TABLE II
COMPARISON OF KEY PARAMETERS BETWEEN MATHEMATICAL AND SIMULATED MODELS

| | **Mathematical Model** | **LTSpice** | **Percentage Difference** |
|---|---|---|---|
| $I_{\rm src}$ | 5.195 A | 5.191 A | 0.0770% |
| $I_{\rm pri}$ | 17.32 A | 17.33 A | −0.0115% |
| $I_{\rm int}$ | 18.71 A | 18.70 A | 0.214% |
| $I_{\rm sec}$ | 11.84 A | 11.84 A | 0% |
| $P_{\rm in}$ | 1064 W | 1063 W | 0.0752% |
| $P_{\rm out}$ | 1000 W | 1000 W | 0% |
| Efficiency | 93.99% | 94.07% | −0.0755% |

### *D. Model Validation With LTspice*

To validate the mathematical model, the circuit shown in Fig. 6(a) was simulated in LTspice with the parameters listed in Table I.

The values for key parameters were solved with the mathematical model as well as with the LTspice model and the results are presented in Table II. The values for the LTspice model were collected at steady state. It can be seen that there is very little difference between the mathematical model and the LTspice simulation at steady state.

### *E. Magnetic Modeling*

With the complexity of (20) and the equations leading to it, it appears to be best not to simplify the model. Instead, a wide range of three coil system designs which may be of interest will be considered.

As noted earlier, a 420-mm-circular pad with its dimensions listed in [22] was used as the base pad for both the primary and secondary pads. The ferrite bars used were made of EPCOS N87 material and the litz wire used had 810 strands of 0.1-mm diameter wire. The original primary coil design was removed and a variety of different primary and intermediate coupler winding designs have been investigated. In all the simulated designs a total of 12 turns of 4-mm diameter copper wire was used to construct both the primary and intermediate coupler windings. The secondary pad was not changed. The primary and secondary pads were aligned at their centers and separated with a pad to pad air gap of 100 mm between them.

In total 62 models were simulated in JMAG with various combinations of primary and intermediate coil locations. Primary coils with one, four, six, eight and 11 turns were simulated while maintaining a total of 12 turns for both the primary and

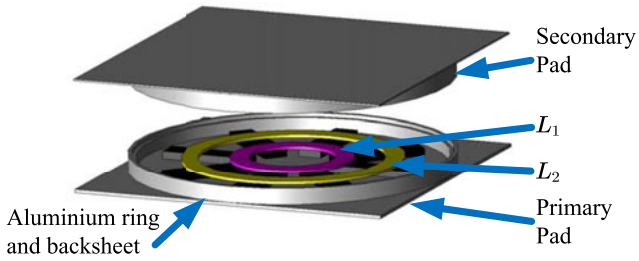


Fig. 8. Pad configuration in JMAG.

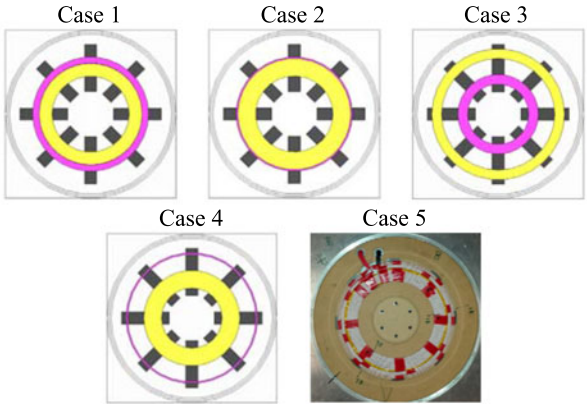


Fig. 9. Primary pad layout of five cases of interest.

intermediate coupler coils. Simulations with the primary coil placed either inside or outside the intermediate coupler coil were also tried. The configuration of the primary and secondary pads is shown in Fig. 8.

The magnetic simulations were run in JMAG Designer 10.0.5 and the inductances of the windings and coupling factors between the windings were measured. The resistance of each coil is assumed to be 0.0146 Ω for every meter of litz wire used. This is the average resistance per meter that was measured when the wire was placed *in situ* within the pad using an Agilent E4980A LCR meter set to 85 kHz. This resistance represents both the AC resistance of the winding as well as the losses in the ferrite. It is also assumed that the ferrite does not saturate under normal operation.

In this study five cases of particular interest are discussed as described in the following sections. The structures of the primary pads are shown in Fig. 9 with the measured parameters presented in Table III. The magenta coil is the primary coil ($L_1$) while the yellow coil is the intermediate coupler winding ($L_2$).

The first four cases are pads which have been simulated in JMAG so they used identical secondary pads. Case 5 is an experimental system that was wound with similar dimensions to Case 1. The secondary winding for the experimental pad was wound in a four turn trifilar fashion. This reduces the inductance of $L_3$ in Case 5 so that an existing high power resistor array could be used as an AC load for the experimental system. The total volume of copper in the secondary pad of the experimental system is still equivalent to the 12 turns of a single-filar coil as

TABLE III
SYSTEM PARAMETERS FOR CASES OF INTEREST

| | Case1 | Case 2 | Case 3 | Case 4 | Case 5 |
|---|---|---|---|---|---|
| $L_1$ ($\mu$H) | 10.4 | 0.78 | 15.2 | 0.71 | 12.1 |
| $L_2$ ($\mu$H) | 32.3 | 56.5 | 20.2 | 47.2 | 33.3 |
| $L_3$ ($\mu$H) | 66.5 | 66.5 | 66.5 | 66.5 | 8.17 |
| $r_1$ (m$\Omega$) | 49 | 13 | 47 | 15 | 44 |
| $r_2$ (m$\Omega$) | 81 | 118 | 83 | 98 | 65 |
| $r_3$ (m$\Omega$) | 130 | 130 | 130 | 130 | 22 |
| $k_{12}$ | 0.6165 | 0.5990 | 0.2434 | 0.2136 | 0.5732 |
| $k_{13}$ | 0.1145 | 0.1009 | 0.1107 | 0.0782 | 0.1257 |
| $k_{23}$ | 0.1292 | 0.1349 | 0.1054 | 0.1280 | 0.1418 |

seen by $L_3$ being approximately one ninth of the inductance of $L_3$ in Cases 1–4. The two coil equivalent parameters for Cases 1–5 can be calculated by using (5) and (7).

## IV. Tuning Intermediate Coupler and Secondary Coils

Previously mentioned studies have suggested that the intermediate coupler and secondary coils need to be tuned to a frequency different that is different from the driving frequency [7], [8]. However, these studies have relied on simplified models of the intermediate coupler system. Using the model derived in (13)–(16), the tuning frequencies of the intermediate coupler ($f_2$) and secondary pad ($f_3$) can be varied to find the optimal tuning for maximum efficiency. As stated earlier, the driving frequency is kept constant at 85 kHz. All the different designs exhibited the same characteristics—A typical case with parallel–parallel tuning will be examined. The details of the model used can be found in Table III under Case 1.

### A. Impact of Tuning on Efficiency

Fig. 10 shows the efficiency of the system when $f_2$ and $f_3$ are varied with no source resistance. The optimal frequency for tuning the intermediate coupler was always found to be higher than the driving frequency. The exact intermediate coupler frequency is by determined by the resistances $r_1$, $r_2$ and $r_3$ as well as the structure of the primary and intermediate coupler coils. Fig. 11 shows how $I_{\mathrm{pri}}$ and $I_{\mathrm{int}}$ vary as the tuning of the intermediate coupler is adjusted when the output power is fixed at 1 kW with a loaded $Q$ factor of 5.

The intermediate coupler tuned frequency can be detuned from the driving frequency $f$ thereby decreasing $I_{\mathrm{int}}$ and increasing $I_{\mathrm{pri}}$ as shown in Fig. 11. This minimizes the total losses in the primary pad since $r_1$ is 41 m$\Omega$ compared to $r_2$ being 81 m$\Omega$ and as seen in Fig. 10 has resulted in the optimal $f_2$ being 96.7 kHz for this system. The system is still tolerant to changes in $f_2$ by more than $\pm$ 5 kHz. A similar observation can also be made with the tuning of the secondary coil.

In almost all feasible cases it was found that, regardless of the frequency the intermediate coupler is tuned to, the optimal $f_3$ is approximately 86 kHz which is only slightly higher than the driving frequency. This is because the losses in the secondary pad cause the optimal $f_3$ to be higher than the driving frequency. Tuning the secondary to 85 kHz has a negligible reduction in

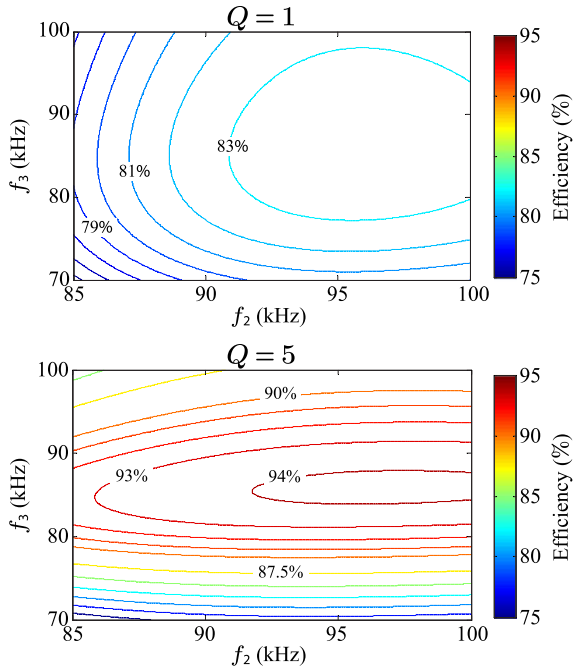


Fig. 10. Efficiency contours of a three coil system at $Q = 1$ and $Q = 5$.

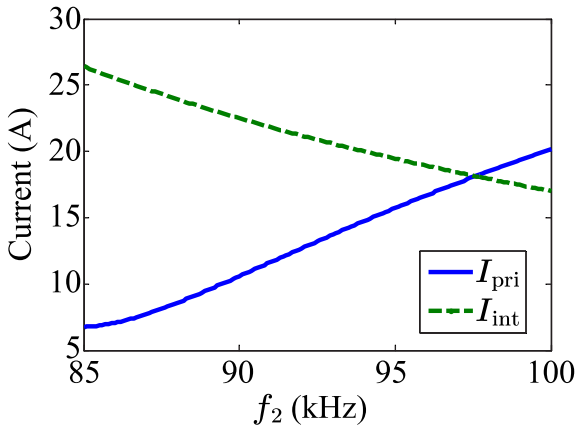


Fig. 11. Variation in $I_{\mathrm{pri}}$ and $I_{\mathrm{int}}$ as the intermediate coupler is detuned.

efficiency (<0.1%). The equivalent two coil system also exhibits exactly the same behavior as shown in Fig. 12 and hence in the majority of cases the secondary pad can be left tuned to 85 kHz.

In a few (mostly impractical) cases such as Case 4 which has a one turn primary, $r_1 = 15$ mΩ, $r_2 = 130$ mΩ, it was found that the optimal $f_3$ was higher (at 90.17 kHz). In such cases, if $f_3$ was set to 85 kHz it would reduce the system efficiency by more than 1.5% which is no longer an insignificant amount. A similar trend can be observed with Case 2 once the source resistances are included but this will be discussed in Sections V and VI.

### B. Impact of Source Losses on Efficiency

The magnitude of the source resistance will impact on the optimal tuning in a similar manner to the way the magnitudes

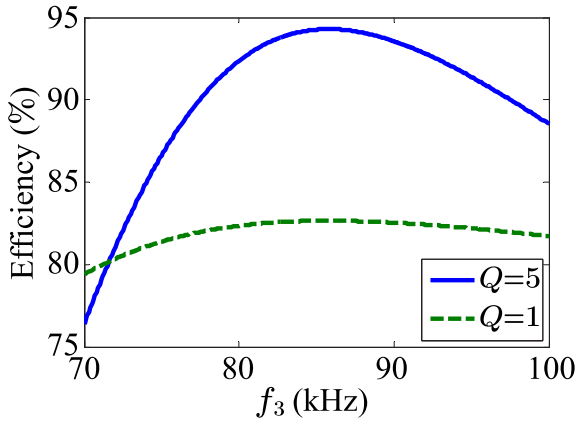


Fig. 12. Two coil equivalent system efficiency at $Q = 1$ and $Q = 5$.

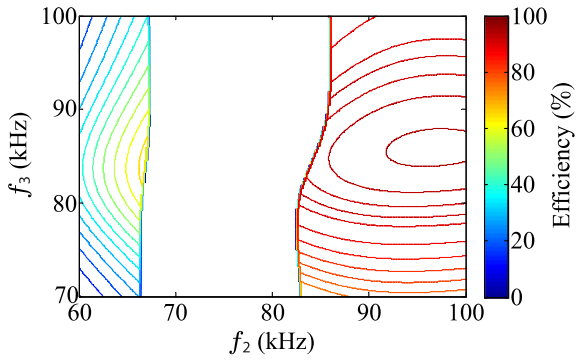


Fig. 13. Capacitive region to be avoided from 65–85 kHz.

of $r_1$, $r_2$ and $r_3$ impacted the optimal tuning of the system. Depending on the tuning topology and size of the source losses, the $f_2$ and $f_3$ can be adjusted to adjust both the primary and intermediate coupler coil currents as well as the source current. This means if the source resistance is very large, the optimal tuning will favor having a lower source current and increasing the intermediate coupler current. The full impact of source losses and how they impact the tuning is investigated in Sections V and VI.

### C. Capacitive-Reflected Impedance of Intermediate Couplers

One precaution to take while tuning the intermediate coupler is to ensure that $f_2$ is higher than $f$ for both parallel–parallel and series–series tuned systems. This is because when $f_2 < f$ the reflected impedance of the tuned intermediate coupler will appear capacitive, potentially causing the effective impedance of the primary coil to also appear capacitive as indicated by the empty region from approximately 65–85 kHz in Fig. 13. This is a similar approach to that taken by many designers who select the tuning of the primary pad to ensure it always presents an inductive load on the H-bridge under all practical operating conditions [25]–[29].

TABLE IV
SIMULATION RESULTS FOR PARALLEL–PARALLEL TUNING TOPOLOGY WITH (A) $R_{\rm src} = 0\ \Omega$, (B) $R_{\rm src} = 0.08\ \Omega$ AND (C) $R_{\rm src} = 0.2\ \Omega$

| | Case 1 | Case 2 | Case 3 | Case 4 | Case 5 |
|---|---|---|---|---|---|
| | | | (a) $R_{\rm src} = 0$ | | |
| $\eta_{\rm NoInt}$ (%) | 86.25 | 60.53 | 89.39 | 42.55 | 89.48 |
| $\eta_{3\text{-coil}}$ (%) | 94.19 | 93.60 | 92.57 | 88.64 | 94.89 |
| $I_{\rm pri}$ (A) | 16.98 | 29.42 | 28.57 | 61.37 | 15.16 |
| $I_{\rm src}$ (A) | 5.22 | 23.40 | 4.10 | 37.24 | 5.33 |
| $I_{\rm int}$ (A) | 18.86 | 18.18 | 16.49 | 24.15 | 17.25 |
| $I_{\rm sec}$ (A) | 11.87 | 11.79 | 11.92 | 10.81 | 33.14 |
| $f_1$ (kHz) | 127.5 | 210.7 | 90.98 | 109.1 | 125.0 |
| $f_2$ (kHz) | 96.69 | 87.56 | 98.90 | 86.86 | 96.55 |
| $f_3$ (kHz) | 85.85 | 86.15 | 85.65 | 90.17 | 86.82 |
| $\eta_{2\text{-coil}}$ (%) | 94.29 | 94.28 | 92.51 | 93.65 | 94.99 |
| $I_{\rm pri\_2}$ (A) | 17.91 | 17.93 | 21.80 | 20.90 | 16.07 |
| $I_{\rm src\_2}$ (A) | 1.70 | 1.71 | 2.13 | 1.91 | 1.79 |
| $I_{\rm sec\_2}$ (A) | 11.90 | 11.90 | 11.95 | 11.92 | 33.28 |
| $f_{1\_2}$ (kHz) | 84.95 | 84.95 | 84.88 | 84.90 | 85.44 |
| $f_{3\_2}$ (kHz) | 85.75 | 85.75 | 85.55 | 85.65 | 86.64 |
| | | | (b) $R_{\rm src} = 0.08$ | | |
| $\eta_{\rm NoInt}$ (%) | 86.15 | 59.59 | 89.33 | 41.93 | 89.39 |
| $\eta_{3\text{-coil}}$ (%) | 94.00 | 90.35 | 92.45 | 82.43 | 94.69 |
| $I_{\rm pri}$ (A) | 17.32 | 34.41 | 28.80 | 70.06 | 15.69 |
| $I_{\rm src}$ (A) | 5.19 | 20.43 | 4.06 | 29.66 | 5.25 |
| $I_{\rm int}$ (A) | 18.71 | 18.87 | 16.26 | 23.93 | 17.05 |
| $I_{\rm sec}$ (A) | 11.84 | 11.06 | 11.92 | 10.43 | 32.98 |
| $f_1$ (kHz) | 126.5 | 181.4 | 90.86 | 107.9 | 123.4 |
| $f_2$ (kHz) | 97.09 | 89.97 | 99.20 | 88.36 | 97.24 |
| $f_3$ (kHz) | 85.95 | 89.06 | 85.65 | 91.87 | 87.04 |
| $\eta_{2\text{-coil}}$ (%) | 94.27 | 94.26 | 92.48 | 93.62 | 94.97 |
| | | | (c) $R_{\rm src} = 0.2$ | | |
| $\eta_{\rm NoInt}$ (%) | 86.02 | 58.24 | 89.24 | 41.04 | 89.25 |
| $\eta_{3\text{-coil}}$ (%) | 93.71 | 86.97 | 92.28 | 76.69 | 94.41 |
| $I_{\rm pri}$ (A) | 17.85 | 38.78 | 29.15 | 80.52 | 16.43 |
| $I_{\rm src}$ (A) | 5.15 | 17.75 | 4.04 | 25.96 | 5.13 |
| $I_{\rm int}$ (A) | 18.45 | 21.24 | 15.95 | 24.78 | 16.81 |
| $I_{\rm sec}$ (A) | 11.81 | 10.34 | 11.90 | 10.05 | 32.73 |
| $f_1$ (kHz) | 125.0 | 175.5 | 90.72 | 106.4 | 121.5 |
| $f_2$ (kHz) | 97.69 | 90.87 | 99.70 | 89.16 | 98.19 |
| $f_3$ (kHz) | 86.05 | 92.27 | 85.75 | 93.68 | 87.39 |
| $\eta_{2\text{-coil}}$ (%) | 94.24 | 94.23 | 92.43 | 93.36 | 94.94 |

## V. EFFICIENCY COMPARISONS USING A PARALLEL–PARALLEL TUNING TOPOLOGY

### A. Test Conditions

The efficiencies of all the primary pad designs were calculated using the model presented in Section III. The system parameters for the five cases that were considered are presented in Table III. As discussed earlier, the model was solved with $R_{\rm src} = 0, 0.08$ and 0.2 to identify the impact it has on the system, and these results are listed in Table IV(a)–(c). In all the cases was operated at $Q = 5$. The driving frequency $f$ was set to 85 kHz. The output power was set to 1 kW by adjusting the primary current $I_{\rm pri}$ as necessary.

The first efficiency listed in the Table IV(a)–(c) is the efficiency of the three coil system but ignoring the intermediate coupler ($\eta_{\rm NoInt}$). For example in Case 2, it would be the efficiency of the system if the primary pad had just a one turn primary coil and no other copper in the pad. The efficiency of the three coil system ($\eta_{3\text{-coil}}$) was calculated when the intermediate coupler was tuned to $f_2$ and the secondary pad was tuned to $f_3$ which are the optimal frequencies to tune the intermediate coupler and secondary pad in order to maximize the efficiency. Finally, the two coil equivalent system efficiency ($\eta_{2\text{-coil}}$), is the system efficiency if $L_1$ and $L_2$ are driven in series by the power supply as described in Section III-A. The two coil equivalent system currents $I_{\rm pri\_2}$, $I_{\rm src\_2}$ and $I_{\rm sec\_2}$ as well the primary and secondary tuning frequencies $f_{1\_2}$ and $f_{3\_2}$ are not listed in Table IV(b) and (c) because they vary by insignificant amounts as $R_{\rm src}$ changes.

### B. Effects of Intermediate Couplers

The first obvious trend that can be observed is that adding extra copper to the primary pad increased the system efficiency as observed by the increase in efficiency from $\eta_{\rm NoInt}$ to $\eta_{3\text{-coil}}$ and $\eta_{2\text{-coil}}$ in all five cases. This result is expected because extra current carrying windings in the primary pad will boost the magnetic flux generated between the primary and secondary pads and hence boost the coupling between the two pads slightly.

When comparing $\eta_{3\text{-coil}}$ to $\eta_{2\text{-coil}}$, there is a much smaller difference in efficiency. With most of the structures, $\eta_{2\text{-coil}}$ was found to be higher than $\eta_{3\text{-coil}}$, as shown in Cases 1, 2, 4 and 5. Some structures were found where $\eta_{3\text{-coil}}$ was higher than $\eta_{2\text{-coil}}$ such as in Case 3 but in these structures $\eta_{3\text{-coil}}$ was higher by negligible amounts. To increase $\eta_{\rm NoInt}$ to equal $\eta_{3\text{-coil}}$, $k_{13}$ (see Table III) would have to be increased significantly. For example in Case 1, $k_{13}$ will need to be boosted to 0.2067 (80% increase) which is in line with the observations in [8]. However, adding the extra copper to the primary pad only boosts the coupling between the primary and secondary pads ($k_{13\_2}$) to 0.1365 (19% increase) while maintaining the same efficiency.

Case 5 shows a pad which was constructed in the lab and was based on the coil structure shown in Case 1 which was found to be the best structure. Using the measured parameters for Case 5 with the mathematical model of the system showed once again that the efficiencies of Case 1 and Case 5 are very similar.

To ensure that $V_{\rm AC}$ sees a purely resistive load, $L_1$ and $L_{1\_2}$ are tuned to $f_1$ and $f_{1\_2}$, respectively, by the variable capacitor $C_1$. It can be seen that $f_1$ varies a lot depending on the structure of the pad and is a lot higher than the driving frequency of 85 kHz. This is due to the large inductive-reflected impedance of the intermediate coupler increasing the effective inductance of the pad during operation. However, the $f_{1\_2}$ values only vary slightly around the 85-kHz driving frequency of the power supply, as expected of a two coil IPT system with low coupling between the primary and secondary pads.

### C. Effects of Varying Coupling

In general, the difference between $\eta_{3\text{-coil}}$ and $\eta_{2\text{-coil}}$ was small when $L_1$ had a strong coupling to either $L_2$ and/or $L_3$. This can be seen in Cases 2 and 3. In Case 2, $L_1$ had weak coupling to $L_3$ but strong coupling to $L_2$ which had a strong coupling to $L_3$ resulting in high $\eta_{3\text{-coil}}$. In Case 3, $L_1$ had low coupling to $L_2$ but both $L_1$ and $L_2$ were fairly strongly coupled to $L_3$ resulting in high $\eta_{3\text{-coil}}$ once again.

However, in Case 4 there is a large difference between $\eta_{3\text{-coil}}$ and $\eta_{2\text{-coil}}$ because the coupling from $L_1$ to $L_2$ and $L_3$ is very low. There is nearly no coupling between $L_1$ and $L_3$ so $L_1$ will

couple power to $L_2$ which couples power to $L_3$. This pathway is very inefficient since there is only one current carrying turn of wire coupling power to $L_2$ so a large current will be required in $L_1$ to deliver the same amount of power as the other cases. To compensate for this $f_2$ approaches 85 kHz in order to minimize the primary current and $f_3$ is heavily mistuned but larger losses in $L_1$ result in low $\eta_{3\text{-coil}}$. However, $\eta_{2\text{-coil}}$ is still high in Case 4 because the power supply is directly driving $L_2$ which couples well to $L_3$ instead of inefficiently coupling power from $L_1$ to $L_2$ with the three coil system.

### D. Effects of Source Resistance

As the source resistance is increased, the system efficiency decreases in both the three coil and two coil equivalent systems. With a three coil system, the optimal tuning of the three coil system changes so that $I_{\text{src}}$ is reduced. This is achieved by lowering the effective primary coil inductance seen by the power supply by detuning the intermediate coupler and secondary coil, resulting in a larger primary tuning capacitor. The overall effect of this is that circulating current in the LC tank increases as seen by the increase in $I_{\text{pri}}$ but the source current decreases. Since the values of $R_{\text{src}} = 0.08\ \Omega$ and $0.2\ \Omega$ is greater than $r_1$ in all five cases, this adjustment in tuning results in a higher efficiency.

The efficiency of the two coil system also decreased as the source resistance increased but by a much smaller amount than the three coil system. The largest change in two coil system efficiency as $R_{\text{src}}$ was increased from 0 to $0.2\ \Omega$ was 0.29% with Case 4. Also, the currents flowing through the system and the tuned frequencies changed by negligible amounts. This is because the only variable that could be adjusted is the secondary tuning and detuning a two coil system further would make the system more inefficient.

However in the aforementioned analysis, the output voltage of the AC source varies significantly between the three coil system and its two coil equivalent. In Case 1 with $R_{\text{src}} = 0.2\ \Omega$, the AC source outputs 206 V at 5.15 A for the three coil system and outputs 626 V at 1.70 A for the two coil equivalent system. The source current is significantly lower for the two coil equivalent system than the three coil system since the effective primary inductance that the AC source drives is much larger with the two coil equivalent system.

In a practical system the voltage of the AC source may need to be constrained to prevent exceeding the maximum voltage rating of the switch by series compensating the primary coil inductance. As discussed earlier in Section II-B, series compensating the primary coil will not change the primary coil current or the output power since it is assumed that $C_1$ is adjusted to keep the power supply perfectly tuned. However, the source current will increase, resulting in higher source losses and lower system efficiency.

The impact of series compensation on efficiency can be investigated by series compensating the primary coil of the two coil equivalent system so that the tank voltage ($V_{\text{tank}}$) shown in Fig. 14(a) is equal to the tank voltage of the optimally tuned three coil system shown in Fig. 14(b). The results of source compensating Cases 1 and 3 are shown in Table V where $\eta_{3\text{-coil}}$ is the three coil system efficiency from Table IV, $\eta_{2\text{-coilsercomp}}$ is the efficiency of the two coil system after it has been series compensated. $I_{\text{src\_2\_sercomp}}$ is the source current of the series-compensated two coil equivalent system.

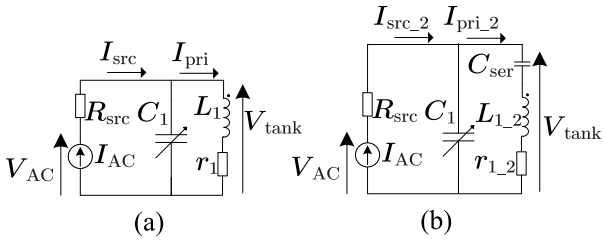


Fig. 14. (a) Primary side of a three coil system and (b) series-compensated primary side of a two coil equivalent system.

TABLE V
IMPACT OF SERIES COMPENSATION OF PARALLEL–PARALLEL-TUNED TOPOLOGY WITH CASES 1 AND 3

| | **Case 1** | **Case 3** |
|---|---|---|
| $R_{\text{src}} = 0.08\ \Omega$ | | |
| $\eta_{3\text{-coil}}$ (%) | 94.00 | 92.45 |
| $\eta_{2\text{-coilsercomp}}$ (%) | 94.10 | 92.40 |
| $I_{\text{src\_2\_sercomp}}$ (A) | 5.19 | 4.08 |
| $R_{\text{src}} = 0.2\ \Omega$ | | |
| $\eta_{3\text{-coil}}$ (%) | 93.71 | 92.28 |
| $\eta_{2\text{-coilsercomp}}$ (%) | 93.82 | 92.23 |
| $I_{\text{src\_2\_sercomp}}$ (A) | 5.14 | 4.04 |

It can be seen that the two coil system efficiency ($\eta_{2\text{-coil}}$) listed in Table IV has decreased after being series compensated. $I_{\text{src\_2\_sercomp}}$ has also increased to be approximately equal to $I_{\text{src}}$ resulting in the source losses of the three coil system to be almost equal to the source losses of the two coil series-compensated system. This results in the difference between $\eta_{3\text{-coil}}$ and $\eta_{2\text{-coilsercomp}}$ following the same trend as what is observed when comparing just the magnetic losses as shown by the comparison between $\eta_{3\text{-coil}}$ and $\eta_{2\text{-coil}}$ when $R_{\text{src}} = 0$ in Table IV(a).

Series compensation Cases 2 and 4 is more difficult due to the large difference between $I_{\text{pri}}$ and $I_{\text{pri\_2}}$. It is not possible to directly series compensate the two coil equivalent system in these cases due to the large reflected resistance of the two coil system. The two coil equivalent system would need to be wound in a bifilar fashion to reduce $I_{\text{pri\_2}}$ so it is approximately equal to $I_{\text{pri}}$ before it is series compensated. Under ideal bifilar conditions where the inductance and series resistance decreases by exactly one quarter, the same trend is observed as was noted with Cases 1 and 3 where the results are comparable to the $R_{\text{src}} = 0$.

## VI. ANALYSIS WITH SERIES–SERIES-TUNED TOPOLOGIES

Several studies have used an intermediate coupler with series–series-tuned systems. The analysis performed in Section V was repeated under the same conditions with a series–series system

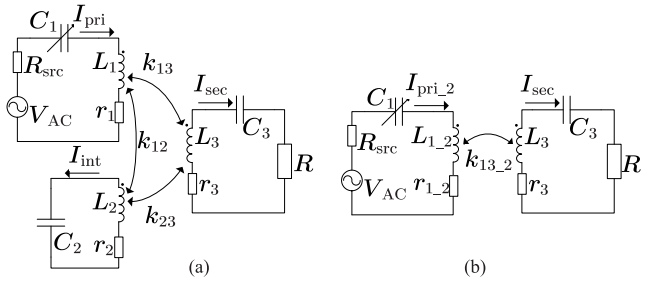


Fig. 15. Series–series-tuned systems with losses in the (a) three coil configuration and (b) its two coil equivalent system.

to see if there is any benefit of having a three coil system over its two coil equivalent system.

### A. Modified System Model

The system model presented in (11)–(16) will be modified to represent a three coil series–series-tuned system and its two coil equivalent system shown in Fig. 15(a) and (b), respectively.

The high frequency AC primary current for the primary coil is supplied by the power supply in a series-tuned system as shown in Fig. 15. This means that losses due to the source are in series with the primary coil, effectively lowering the quality factor of the primary coil by a significant amount. To get around this problem, an intermediate coupler coil with a high quality factor was used in several series–series systems [21] allowing a large current to flow through the intermediate coupler coil while maintaining minimal losses. Therefore, for this method to be effective the primary current for a three coil system $I_{\rm pri}$ has to be lower than the primary current of the two coil equivalent system $I_{\rm pri\_2}$ to minimize source losses.

To account for the different source loss, the efficiency equation (20) has been modified to

$$\eta = \frac{P_{\rm out}}{r_{\rm src} I_{\rm pri}^2 + \Re\left(V A_{\rm pri}\right)}. \tag{21}$$

Modifying the system equations to account for a series-tuned secondary coil will have minimal effect on the efficiency comparison between a three coil system and its two coil equivalent systems. This is because the losses due to the series-tuned secondary will be constant in both systems since the output power and $Q$ is fixed unless the secondary pad is heavily mistuned. To allow for a series-tuned secondary, the secondary tuning factor $a_3$ in equations (11)–(14) is modified to

$$a_3 = -\left(1 + \frac{\omega_3^2}{\omega^2} - \frac{j}{Q} + \frac{r_3}{j\omega L_3}\right). \tag{22}$$

The load current is now given by

$$I_R = I_{\rm sec}. \tag{23}$$

### B. Series–Series Efficiency Comparisons

The series–series model was run with the same test conditions listed in Section V-A with the same system parameters listed in Table III. The results of the series–series simulations are listed in Table VI in the same format as Table IV. The series–series system also exhibits the same general trends as the parallel–parallel system—most notably the $\eta_{3\text{-coil}}$ and $\eta_{2\text{-coil}}$ being significantly higher than $\eta_{\rm NoInt}$ due to the extra copper current carrying turns being added into the primary pad. Also, when operating with $R_{\rm src} = 0$, the difference between $\eta_{3\text{-coil}}$ and $\eta_{2\text{-coil}}$ was very small in most cases—just like a parallel–parallel system with no source resistance.

However, once the source resistance is introduced the efficiency of the system reduced dramatically in most cases. In all five cases the $f_2$ approached 85 kHz in order to decrease $I_{\rm pri}$ and increase $I_{\rm int}$ so that the effect of the source losses are minimized. With the one turn primary coil systems (Cases 2 and 4), the $f_3$ was also heavily mistuned however $I_{\rm pri}$ was still larger than $I_{\rm pri\_2}$, resulting in the three coil system being significantly less efficient than its two coil equivalent system. However, for Cases 1, 3 and 5, $I_{\rm pri}$ was significantly smaller than $I_{\rm pri\_2}$, resulting in $\eta_{3\text{-coil}}$ being higher than $\eta_{2\text{-coil}}$ due to minimal source losses. The systems with high mutual inductance between the primary and intermediate coil (Cases 1, 3 and 5) also tended to

TABLE VI
SIMULATION RESULTS FOR SERIES–SERIES TUNING TOPOLOGY WITH (A) $R_{\rm src} = 0\ \Omega$, (B) $R_{\rm src} = 0.08\ \Omega$ AND (C) $R_{\rm src} = 0.2\ \Omega$

| | Case 1 | Case 2 | Case 3 | Case 4 | Case 5 |
|---|---|---|---|---|---|
| (a) $R_{\rm src} = 0$ | | | | | |
| $\eta_{\rm NoInt}$ (%) | 86.29 | 60.56 | 89.44 | 42.57 | 89.54 |
| $\eta_{3\text{-coil}}$ (%) | 94.22 | 93.64 | 92.62 | 88.73 | 94.90 |
| $I_{\rm pri}$ (A) | 16.93 | 29.32 | 28.42 | 61.33 | 14.98 |
| $I_{\rm src}$ (A) | 16.93 | 29.32 | 28.42 | 61.33 | 14.98 |
| $I_{\rm int}$ (A) | 18.76 | 18.03 | 16.47 | 23.26 | 16.89 |
| $I_{\rm sec}$ (A) | 11.86 | 11.86 | 11.86 | 11.86 | 33.85 |
| $f_1$ (kHz) | 122.0 | 127.4 | 90.63 | 86.26 | 116.6 |
| $f_2$ (kHz) | 97.19 | 87.96 | 99.50 | 87.46 | 96.67 |
| $f_3$ (kHz) | 85.05 | 85.25 | 85.05 | 88.86 | 85.08 |
| $\eta_{2\text{-coil}}$ (%) | 94.33 | 94.32 | 92.56 | 93.69 | 95.00 |
| $I_{\rm pri\_2}$ (A) | 17.85 | 17.86 | 21.75 | 20.84 | 15.81 |
| $I_{\rm sec}$ (A) | 17.85 | 17.86 | 21.75 | 20.84 | 15.81 |
| $I_{\rm sec\_2}$ (A) | 11.86 | 11.86 | 11.86 | 11.86 | 33.85 |
| $f_{1\_2}$ (kHz) | 85.36 | 85.36 | 85.38 | 85.33 | 85.56 |
| $f_{3\_2}$ (kHz) | 84.95 | 84.95 | 84.95 | 84.95 | 84.95 |
| (b) $R_{\rm src} = 0.08$ | | | | | |
| $\eta_{\rm NoInt}$ (%) | 72.17 | 17.97 | 77.84 | 10.46 | 78.00 |
| $\eta_{3\text{-coil}}$ (%) | 93.13 | 89.40 | 89.10 | 75.72 | 93.99 |
| $I_{\rm pri}$ (A) | 9.81 | 23.10 | 19.26 | 43.12 | 9.13 |
| $I_{\rm src}$ (A) | 9.81 | 23.10 | 19.26 | 43.12 | 9.13 |
| $I_{\rm int}$ (A) | 22.95 | 20.69 | 26.08 | 35.89 | 20.84 |
| $I_{\rm sec}$ (A) | 11.86 | 11.86 | 11.86 | 11.86 | 33.85 |
| $f_1$ (kHz) | 139.7 | 87.18 | 95.43 | 83.23 | 124.7 |
| $f_2$ (kHz) | 90.17 | 86.96 | 91.17 | 86.86 | 89.86 |
| $f_3$ (kHz) | 85.15 | 88.46 | 85.25 | 95.38 | 85.24 |
| $\eta_{2\text{-coil}}$ (%) | 92.11 | 92.10 | 89.42 | 90.74 | 93.23 |
| (c) $R_{\rm src} = 0.2$ | | | | | |
| $\eta_{\rm NoInt}$ (%) | 57.95 | 8.74 | 65.17 | 4.91 | 65.36 |
| $\eta_{3\text{-coil}}$ (%) | 92.38 | 85.32 | 86.49 | 66.08 | 93.28 |
| $I_{\rm pri}$ (A) | 7.67 | 19.67 | 15.05 | 37.47 | 7.66 |
| $I_{\rm src}$ (A) | 7.67 | 19.67 | 15.05 | 37.47 | 7.66 |
| $I_{\rm int}$ (A) | 24.62 | 24.56 | 31.35 | 44.44 | 22.30 |
| $I_{\rm sec}$ (A) | 11.86 | 11.86 | 11.86 | 11.86 | 33.85 |
| $f_1$ (kHz) | 134.6 | 83.04 | 96.39 | 88.73 | 113.7 |
| $f_2$ (kHz) | 87.96 | 87.16 | 88.66 | 86.55 | 88.02 |
| $f_3$ (kHz) | 85.25 | 91.57 | 85.45 | 98.80 | 85.54 |
| $\eta_{2\text{-coil}}$ (%) | 88.98 | 88.96 | 85.10 | 86.64 | 90.69 |

operate with a higher $\eta_{3\text{-coil}}$ than $\eta_{2\text{-coil}}$ which is in line with the results from [13].

Cases 1 and 5 highlight the strengths of a well-designed series–series-tuned three coil system since the $\eta_{3\text{-coil}}$ decreased by just 2% when increasing $R_{\text{src}}$ from 0 to 0.2 Ω while $\eta_{2\text{-coil}}$ decreased by more than 4%. This was due to the significant change in $I_{\text{pri}}$ caused by $f_2$ approaching 85 kHz. In Case 1, $I_{\text{pri}}$ reduced by 45% by retuning the intermediate coupler as the source resistance increased to reduce source losses for the three coil system while $I_{\text{pri\_2}}$ remained constant for all source resistance values, causing very large source losses in the two coil equivalent system. The 1:2 ratio used for the width of the primary coil to the intermediate coil in Cases 1 and 5 also match the optimal ratio range observed in [13].

### C. Differences Between Parallel–Parallel and Series–Series Tuned Systems

Due to topology differences between series and parallel tuned power supplies and other realistic limitations such as maximum voltage limits within the system, it would not be valid to compare the parallel–parallel efficiencies listed in Table IV to the series–series efficiencies listed in Table VI. Parallel–parallel-tuned systems using current-sourced supplies often have dc inductors [4] whilst voltage-sourced supplies are typically driven through an additional AC inductor [30] which effectively increase the source resistance of the system. Regardless of this, general observations of trends in the data can still be made.

Series–series-tuned systems appear to work most efficiently when using an independently tuned intermediate coil. This result is confirmed by several previous works which have also used intermediate coupler structures with series–series systems. However, this comes at the cost of making the tuning of the system more complicated since the optimal tuning frequency of the primary coil ($f_1$) depends on the intermediate coil configuration and the tuning frequency of the intermediate coupler ($f_2$). If the source impedance is assumed to be large, $f_2$ can simply be fixed at a frequency slightly higher than $f$ and $f_1$ can be tuned appropriately. The series–series-tuned system is significantly more inefficient when driving a two coil IPT system with a large source resistance since $I_{\text{pri\_2}}$ cannot be adjusted like $I_{\text{pri}}$, resulting in significant source losses.

Parallel–parallel-tuned systems work very efficiently when driven as a two coil system. Even Case 4, which exhibited extremely bad performance in all series–series configurations and when driven as a three coil, parallel–parallel-tuned system, achieves relatively good efficiency when driven as a parallel–parallel-tuned two coil system. A lot of the three coil systems were also found to be efficient when driven with a source resistance. However, partial series compensation of a standard two coil parallel–parallel-tuned systems increases the source current and hence the source losses. It is not unreasonable to expect a primary pad to be partially series compensated in order to increase the vars of the primary coil. Under the worst case partial series compensation, there is barely any difference in efficiency between the three coil system and its two coil equivalent system.

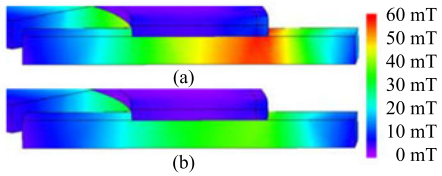


Fig. 16. Cross section of pad indicating (a) magnetic flux hotspot in the ferrites for a three coil system and (b) even magnetic flux distribution when driven as a two coil system.

The three coil system requires complicated tuning based on the design of the primary pad to achieve the maximum efficiency whereas the primary and secondary coils in the two coil systems are simply tuned to 85 kHz regardless of which pad or source efficiency was considered.

There are however other issues to investigate which are beyond the scope of this study, such as how sensitive these systems are to mistuning (which was briefly commented on in Section IV-A) and the performance of each system under misalignment (as is often the case with EV charging).

## VII. Practical Considerations

### A. Low Efficiency Compared to Other Systems

The systems presented in Cases 1–5 have a very low efficiency considering that only pad losses and source conduction losses have been taken into account. In another study [8], a full system with an intermediate coupler was shown to run at 95.57% efficiency. Here, the intent of this study was not to build a high efficiency system but to investigate intermediate couplers and validate the models using small 420-mm diameter pads which are more convenient to test. To increase the efficiency of the system, pads designed specifically for 85 kHz have to be made. The circular pads used in this study only have a coil quality factor of approximately 280 but if the copper and ferrite design was optimized, quality factors of 400–600 can be achieved which would significantly reduce the pad losses.

### B. Magnetic Flux Distribution

An intermediate coupler system such as Case 2 in Table III can be used where the single turn primary coil has a very low inductance and is much easier to drive. However, this will create a large difference in currents between $I_{\text{pri}}$ and $I_{\text{int}}$ as shown in Table IV. The large current flowing through the primary coil will create a magnetic flux hotspot in the ferrites of the pad as shown in Fig. 16(a) which may saturate the ferrite at that spot. The 60-mT hotspot in Fig. 16(a) is not enough to saturate typical ferrites, however in larger pads operating at higher power levels saturation may occur. If the equivalent two coil structure was used where constant current flows through the primary pad, a smoother flux distribution is observed in the ferrite as shown in Fig. 16(b).

### C. Similarity to Series-Compensated Primary Coils

The inductance of a parallel–parallel-tuned primary pad can be lowered so that both the three coil system and its partially

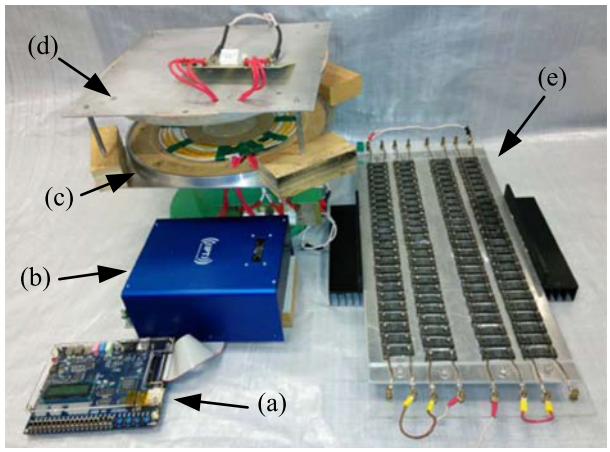


Fig. 17. Experimental setup showing the (a) controller, (b) 85-kHz power supply, (c) primary pad, (d) secondary pad and (e) AC resistor array.

TABLE VII
TUNING CAPACITORS USED FOR EXPERIMENTAL SYSTEM

| **Three coil parameters:** | | **Two coil parameters:** | |
|---|---|---|---|
| $C_{\rm pri}$ | 157 nF | $C_{\rm pri}$ | 149 nF |
| $C_{\rm int}$ | 80 nF | $C_{\rm series}$ | 80.7 nF |
| $C_{\rm sec}$ | 444 nF | $C_{\rm sec}$ | 444 nF |

series-compensated two coil equivalent system require the same value capacitor for $C_1$. At this point there is no practical difference between an efficiently designed parallel–parallel three coil system and its two coil equivalent system. In a three coil system the extra copper introduced as the intermediate coupler coil is tuned out by $C_2$. Similarly, in a partially series-compensated two coil system as shown in Fig. 4, the extra copper ($L_{\rm ser1}$) can be tuned out by the series capacitor $C_{\rm series}$. Both systems exhibit a similar tolerance to mistuning as shown in Figs. 10 and 12. However, it is much simpler to tune a two coil system since both the primary and secondary pads can be tuned to the driving frequency, whereas tuning the primary and intermediate coupler coils in a three coil system is more involved.

## VIII. EXPERIMENTAL RESULTS

The system shown in Case 5 has been energized as a parallel–parallel-tuned system in the laboratory and the efficiency measurements of the three coil system and its two coil equivalent system were recorded. The measured inductances, losses and coupling factors of the system are listed in Table III and the experimental setup is shown in Fig. 17. The tuning capacitances used are listed in Table VII.

A high power resistor array of 16.4 Ω was used as the load so the $Q$ of the secondary is 3.76. The primary coil was driven using a push-pull power supply and the input voltage was increased until the output power was 1 kW.

The comparison between simulated results and the practical measurements are listed in Table VIII and some current waveforms are shown in Fig. 18. The simulated values in Table VIII used the experimental values of $f_2$ and $f_3$ since it was difficult to perfectly tune the intermediate coupler and secondary coils to the optimal frequency. Table VIII presents both the magnetic efficiency ($\eta_{\rm mag}$) of the experimental system as well as the total system efficiency ($\eta_{\rm total}$). The magnetic loss in the experimental system was calculated by using the coil currents from Table VIII and coil ESRs from Table III.

TABLE VIII
SIMULATED VERSUS EXPERIMENTAL SYSTEM CURRENTS

| | **Simulated three-coil** | **Actual three-coil** | **Simulated two-coil** | **Actual two-coil** |
|---|---|---|---|---|
| $I_{\rm pri}$ | 19.6 A | 19.3 A | 18.4 A | 17.9 A |
| $I_{\rm int}$ | 18.2 A | 18.3 A | - | - |
| $I_{\rm sec}$ | 31.7 A | 30.3 A | 31.7 A | 30.0 A |
| $I_R$ | 7.8 A | 7.8 A | 7.8 A | 7.8 A |
| $P_{\rm out}$ | 1000 W | 1014 W | 1000 W | 1006 W |
| $P_{\rm in\_mag}$ | 1057 W | 1073 W | 1056 W | 1060 W |
| $\eta_{\rm mag}$ | 94.3% | 94.5% | 94.4% | 94.9% |
| $P_{\rm in\_total}$ | - | 1111 W | - | 1106 W |
| $\eta_{\rm total}$ | - | 91.3% | - | 91.0% |

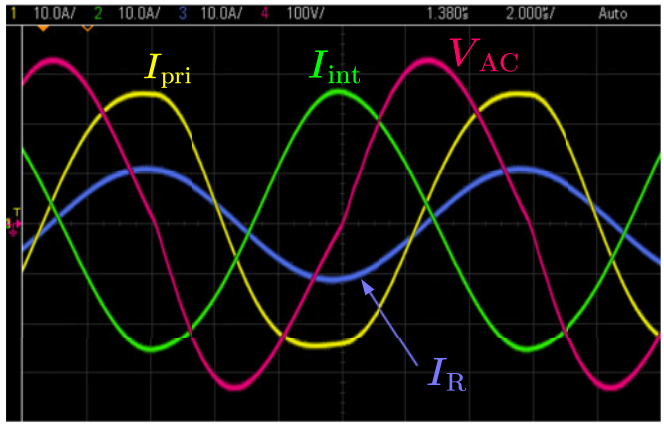


Fig. 18. Oscilloscope measurements during circuit operation. Yellow: $I_{\rm pri}$, green: $I_{\rm int}$, blue: $I_{\rm R}$, pink: $V_{\rm AC}$.

The simulated and experimental values for the currents and $\eta_{\rm mag}$ are very similar suggesting that the models for the three coil system and the two coil equivalent system are reliable. The total system efficiency for the experimental system was approximately 3% lower than the magnetic efficiency which validates the original model assumption that the pad losses are the highest losses in an IPT system. The practical measurements confirm that there is very little difference in efficiency between a three coil system and its two coil equivalent system for well-designed parallel–parallel-tuned systems.

## IX. CONCLUSION

The addition of extra current carrying windings to a primary pad boosts the coupling to the secondary pad, resulting in higher operating efficiency. Aligning with recent works, it is shown that an independently tuned, coplanar intermediate coupler coil embedded within a primary pad benefits a series–series-tuned

system since it creates an additional var source free of the source loss in the power supply. However, for the system to be perfectly tuned, both the primary and intermediate coupler coils require a complicated tuning method to achieve maximum system efficiency.

In a parallel–parallel-tuned system it is more efficient to drive the pad as a traditional two coil system while tuning out the inductance of the extra copper added to the primary pad with series capacitors if necessary. In parallel-tuned power supplies, the pad inductance and tuned capacitor naturally create a var source free of the source resistance of the power supply. The optimal tuning is much simpler for the two coil system since the primary and secondary coils are only tuned to the driving frequency of the power supply regardless of what pads are used.

Two coil systems also create a more even magnetic flux distribution within the ferrites than the three coil system so that the ferrites in the primary pad are less likely to saturate.

## REFERENCES


[1] G. A. Covic and J. T. Boys, "Modern trends in inductive power transfer for transportation applications," *IEEE J. Emerging Sel. Topics Power Electron.*, vol. 1, no. 1, pp. 28–41, Mar. 2013.

[2] J. Huh, S. W. Lee, W. Y. Lee, G. Cho, and C. T. Rim, "Narrow-width inductive power transfer system for online electrical vehicles," *IEEE Trans. Power Electron.*, vol. 26, no. 12, pp. 3666–3679, Dec. 2011.

[3] O. C. Onar, J. M. Miller, S. L. Campbell, C. Coomer, C. P. White, and L. E. Seiber, "Oak ridge national laboratory wireless power transfer development for sustainable campus initiative," in *Proc. IEEE Transp. Electrification Conf. Expo.*, 2013, pp. 1–8.

[4] A. W. Green and J. T. Boys, "10 kHz inductively coupled power transfer-concept and control," in *Proc. Int. Conf. Power Electron. Variable-Speed Drives*, 1994, pp. 694–699.

[5] G. A. Covic, G. Elliott, O. H. Stielau, R. M. Green, and J. T. Boys, "The design of a contact-less energy transfer system for a people mover system," in *Proc. IEEE Int. Conf. Power Syst. Technol.*, 2000, pp. 79–84.

[6] H. H. Wu, A. Gilchrist, and D. Bronson, "A 90 percent efficient 5kW inductive charger for EVs," in *Proc. IEEE Energy Convers. Congr. Expo.*, 2012, pp. 275–282.

[7] D. Ahn and S. Hong, "A study on magnetic field repeater in wireless power transfer," *IEEE Trans. Ind. Electron.*, vol. 60, no. 1, pp. 360–371, Jan. 2013.

[8] S. C. M. Moon, B. C. Kim, S. Y. Cho, and G. Woo, "Analysis and design of wireless power transfer system with an intermediate coil for high efficiency," *IEEE Trans. Ind. Electron.*, vol. 61, no. 11, pp. 5861–5870, Nov. 2014.

[9] C. K. Lee, W. X. Zhong, and S. Y. R. Hui, "Effects of magnetic coupling of nonadjacent resonators on wireless power domino-resonator systems," *IEEE Trans. Power Electron.*, vol. 27, no. 4, pp. 1905–1916, Apr. 2012.

[10] J. W. Kim, H. C. Son, K. H. Kim, and Y. J. Park, "Efficiency analysis of magnetic resonance wireless power transfer with intermediate resonant coil," *IEEE Antennas Wireless Propag. Lett.*, vol. 10, pp. 389–392, (2011). [Online]. Available: http://ieeexplore.ieee.org/xpl/articleDetails.jsp?arnumber=5762318.

[11] F. Zhang, S. A. Hackworth, W. Fu, C. Li, Z. Mao, and M. Sun, "Relay effect of wireless power transfer using strongly coupled magnetic resonances," *IEEE Trans. Magn.*, vol. 5, no. 47, pp. 1478–1481, May 2011.

[12] M. Kiani, U. M. Jow, and M. Ghovanloo, "Design and optimization of a 3-coil inductive link for efficient wireless power transmission," *IEEE Trans. Biomed. Circuits Syst.*, vol. 5, no. 6, pp. 579–591, Dec. 2011.

[13] W. X. Zhong, C. Zhang, X. Liu, and S. Y. R. Hui, "A methodology for making a 3-coil wireless power transfer system more energy efficient than a 2-coil counterpart for extended transmission distance," *IEEE Trans. Power Electron.*, vol. 30, no. 2, pp. 933–942, Mar. 2014.

[14] J. T. Boys, "Inductive power transfer across an extended gap," N.Z. Patent App. 98/050 993, Jan. 7, 1999.

[15] J. T. Boys, "Power supply for an electroluminescent display," U.S. Patent 6 317 338, Nov. 13, 2001.

[16] J. T. Boys, "Inductively-powered power transfer system with one or more independently controllable loads," U.S. Patent 7 633 235, Dec. 15, 2009.

[17] A. H. Mohammadian, E. T. Ozaki, and M. S. Grob, "Repeaters for enhancement of wireless power transfer," U.S. Patent App. 12/266 520, Nov. 19, 2009.

[18] R. Mobarhan, R. Burdo, and L. N. Bonacci, "Wireless power transfer in public places," U.S. Patent App. 12/572 388, Aug. 12, 2010.

[19] E. R. Giler, K. L. Hall, M. P. Kesler, M. Soljacic, A. Karalis, A. B. Kurs, Q. Li, and S. J. Ganem, "Wireless energy transfer using repeater resonators," U.S. Patent 8 587 155, Nov. 19, 2013.

[20] T. Imura, "Equivalent circuit for repeater antenna for wireless power transfer via magnetic resonant coupling considering signed coupling," in *Proc. IEEE Conf. Ind. Electron. Appl.*, 2011, pp. 1501–1506.

[21] A. P. Sample, D. A. Meyer, and J. R. Smith, "Analysis, experimental results, and range adaptation of magnetically coupled resonators for wireless power transfer," *IEEE Trans. Ind. Electron.*, vol. 58, no. 2, pp. 544–554, Feb. 2011.

[22] M. Budhia, G. A. Covic, and J. T. Boys, "Design and optimization of circular magnetic structures for lumped inductive power transfer systems," *IEEE Trans. Power Electron.*, vol. 26, no. 11, pp. 3096–3108, Nov. 2011.

[23] R. P. Twiname, D. J. Thrimawithana, U. K. Madawala, and C. A. Baguley, "A new resonant bi-directional DC-DC converter topology," *IEEE Trans. Power Electron.*, vol. 29, no. 9, pp. 4733–4740, Sep. 2014.

[24] Y. Xiong, S. Sun, H. Jia, P. Shea, and J. Z. Shen, "New physical insights on power MOSFET switching losses," *IEEE Trans. Power Electron.*, vol. 24, no. 2, pp. 525–531, Feb. 2009.

[25] H. Hao, G. A. Covic, and J. T. Boys, "A parallel topology for inductive power transfer power supplies," *IEEE Trans. Power Electron*, vol. 29, no. 3, pp. 1140–1151, Mar. 2014.

[26] M. L. G. Kissin, H. Hao, and G. A. Covic, "A practical multiphase IPT system for AGV and roadway applications," in *Proc. IEEE Energy Convers. Congr. Expo.*, 2010, pp. 1844–1850.

[27] R. L. Steigerwald, "High-frequency resonant transistor DC-DC converters," *IEEE Trans. Ind. Electron.*, vol. 31, no. 2, pp. 181–191, May 1984.

[28] T. H. Sloan, "Design of high-efficiency series-resonant converters above resonance," *IEEE Trans. Aerosp. Electron. Syst.*, vol. 26, no. 2, pp. 393–402, Mar. 1990.

[29] U. Schwarzer and R. W. De Doncker, "Power losses of IGBTs in an inverter prototype for high frequency inductive heating applications," in *Proc. IEEE Conf. Ind. Electron. Soc.*, 2001, pp. 793–798.

[30] H. Hao, G. A. Covic, and J. T. Boys, "An approximate dynamic model of LCL-T based inductive power transfer power supplies," *IEEE Trans. Power Electron.*, vol. 29, no. 10, pp. 5554–5567, Oct. 2014.


**Abhilash Kamineni** (S'10) received the B.E. (Hons.) degree from the University of Auckland, Auckland, New Zealand, in 2012, where he is currently working toward the Ph.D. degree.

His current research interests include the design and analysis of inductive power transfer systems and developing the power electronics circuits for electric vehicle charging in both stationary and dynamic scenarios.

**Grant A. Covic** (S'88–M'89–SM'04) received the B.E. (Hons.) and Ph.D. degrees in electrical and electronic engineering from the University of Auckland (UoA), Auckland, New Zealand, in 1986 and 1993, respectively.

He was appointed as a Full Time Lecturer in 1992, a Senior Lecturer in 2000, an Associate Professor in 2007 and Professor in 2013 within the Electrical and Computer Engineering Department, UoA. In 2010, he cofounded (with John Boys) a new global start-up company "HaloIPT" focusing on electric vehicle (EV) wireless charging infrastructure, which was sold in late 2011. Presently, he heads power electronics research at the UoA and coleads the interoperability subteam within the SAE J2954 wireless charging standard for EVs.

His research and consulting interests include power electronics, electric vehicle battery charging and inductive (contactless) power transfer (IPT) from which he has published more than 100 refereed papers in international journals and conferences. He holds a number of US patents with many more pending, from which licenses in specialized application areas of IPT have been granted around the world.

Dr. Covic is a Fellow of the Institution of Professional Engineers New Zealand, and (together with Professor Boys) has been awarded the New Zealand Prime Minsters Science Prize, the KiwiNet Research Commercialization Award and the Vice Chancellors Commercialization Medal for his work in IPT.

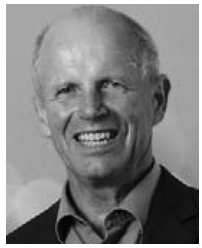

**John T. Boys** received the M.E. degree from the University of Auckland, Auckland, New Zealand, in 1965.

After completing the Ph.D., he was with SPS Technologies for five years before returning to academia as a Lecturer at the University of Canterbury, Christchurch, New Zealand. He moved to Auckland in 1977 where he developed his work in power electronics.

He is currently Distinguished Professor Emeritus at the Department of Electrical and Computer Engineering, University of Auckland, and cofounder of HaloIPT. He has published more than 100 papers in international journals and is the holder of more than 40 US patents from which licenses in specialized application areas have been granted around the world. His research interests include power electronics and electromagnetics for inductive power transfer, where he works with G. A. Covic.

Dr. Boys is a Fellow of the Royal Society of New Zealand and a Distinguished Fellow of the Institution of Professional Engineers New Zealand.